DOI: https://doi.org/10.68732/3115e233b0132296

ISBN: 978-9989-2053-6-1

Time-based hydro-mechanical modelling of tunnelling in weathered granite

L. Zdravkovic & D. M. Potts
Imperial College London, London, UK
l.zdravkovic@imperial.ac.uk
0000-0003-3092-0628

J. H. Shin
Konkuk University, Seoul, South Korea

Abstract

This paper considers the construction practice of NATM tunnelling in a mixed face and water bearing ground profiles comprising different levels of rock degradation. The study is based on the geological conditions of the Seoul subway (South Korea), where the geology around the city comprises a large granite batholith. Deeply weathered granite in this area is frequently encountered in many civil engineering works, including subway construction.

One frequent challenge for tunnel construction is the geological profile which comprises decomposed granite above the tunnel spring-line and weathered granite below. The former is practically a soil while the latter is a transitional zone to the underlying rock, containing parts of residual soils and of partially weathered and/or fresh rock. Another challenge is the design of tunnel linings with the presence of pore water pressures and possible water infiltration into tunnels.

This paper develops a numerical model to investigate and quantify the pore-water pressure and its potential effects on the tunnel lining. It is shown that the development of pore-water pressure on the lining is dependent on the lining permeability and the deterioration of the drainage system, particularly for a tunnel with both a primary and a secondary lining. The magnitude of pore-water pressure on a NATM tunnel constructed in this ground conditions and the effect of tunnel shape are investigated. Design curves for estimating pore-water pressure loads on a secondary lining are proposed.

Keywords

Tunnelling, Weathered rock, Numerical modelling, Lining permeability.

1 Introduction

1.1 Hydraulic conditions

Tunnelling beneath the water table induces pore water pressure changes and alters the hydraulic regime in the ground. This can cause seepage into the tunnel and often produces a long-term interaction between the tunnel and the surrounding soil. According to Peck (1969), one of the requirements for a satisfactory tunnel design is to be capable of withstanding, during its lifetime, all the influences that it may experience. The most critical long-term influences caused by groundwater are leakage and external pore-water pressures on the lining. Water leakage could be particularly problematic for the efficient operation of the tunnel system, and it can lead to the deterioration of various components, especially in rail and highway tunnels. The pathways for water infiltration into the tunnel are usually shrinkage cracks in the concrete lining, construction joints, and cracks due to concrete deterioration or structural failure. The latter are the most dangerous and can cause overall tunnel failure (O'Rourke 1984; Parks et al. 1986).

The New Austrian Tunnelling Method (NATM) was preferred in the Seoul Subway construction, as it allows the excavation profile to cope effectively with the variable ground conditions. A wide range of tunnel shapes was used, from circular/elliptical to horse-shoe shapes. The cases of NATM tunnel failures, associated with pore-water pressures acting on the lining, were reported by Ferreira (1995) and Lee et al. (1996). The tunnels had both a primary and a secondary lining, and structural damage was observed only in the secondary linings. Shin et al. (2002) studied numerically the long-term variation of ground loading on 4 m diameter tunnels constructed 20 m beneath the ground surface. They indicated that the ground loading depended primarily on the nature of the soil and the hydraulic boundary conditions, such as lining and soil permeability. They also showed that the distribution of pore pressure corresponding to long-term seepage depended on the relative permeability of the lining and the surrounding soil/rock. Availability of field measurements of long-term ground and pore pressures is often limited to be able to support validations of numerical models. However, a significant case record was presented by Inokuma and Ishimura (1995), involving measured total soil and water pressures around a concrete segmental lining of a 5 m diameter and a 32 m dep tunnel, which was constructed with a slurry shield in loose clayey silty sands. The data in Fig. 1 show that most of the ground loading was from the pore-water pressure, the effective stress component from the soil itself being small.

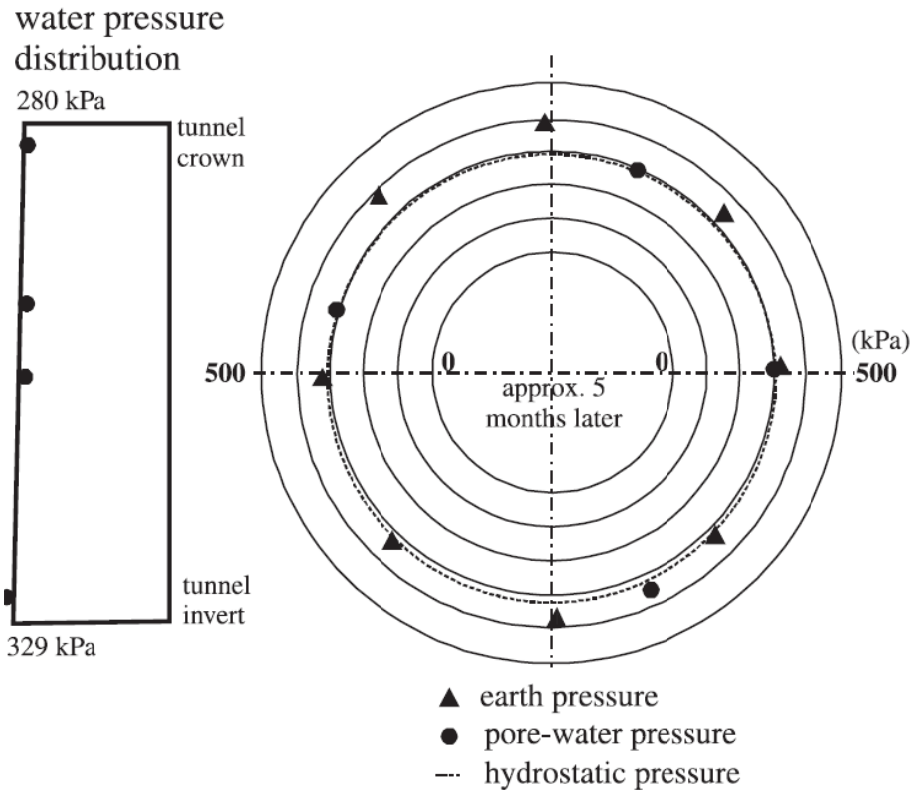
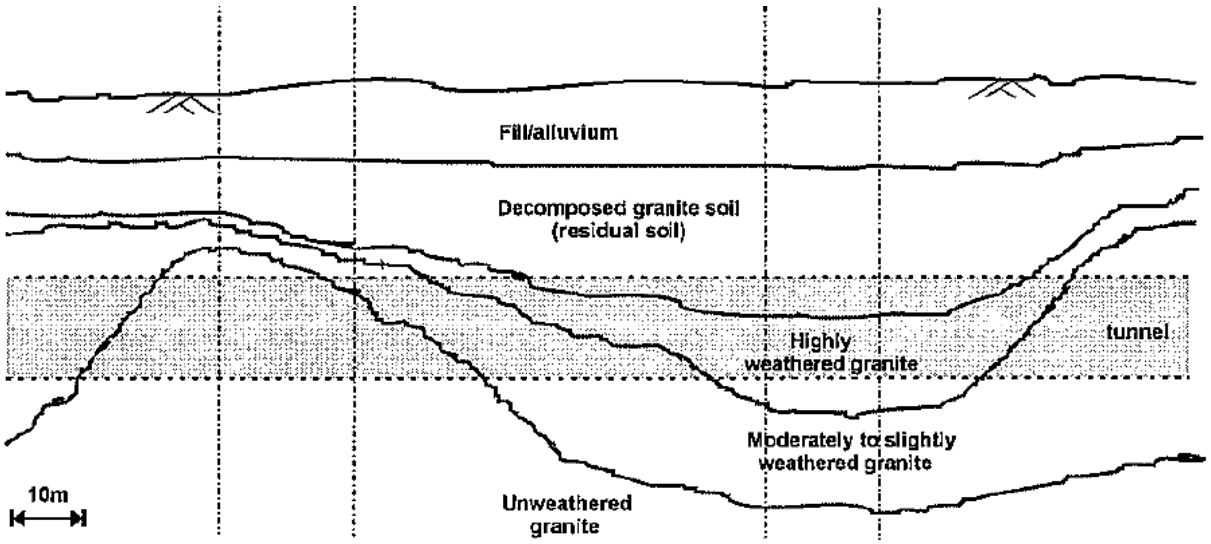


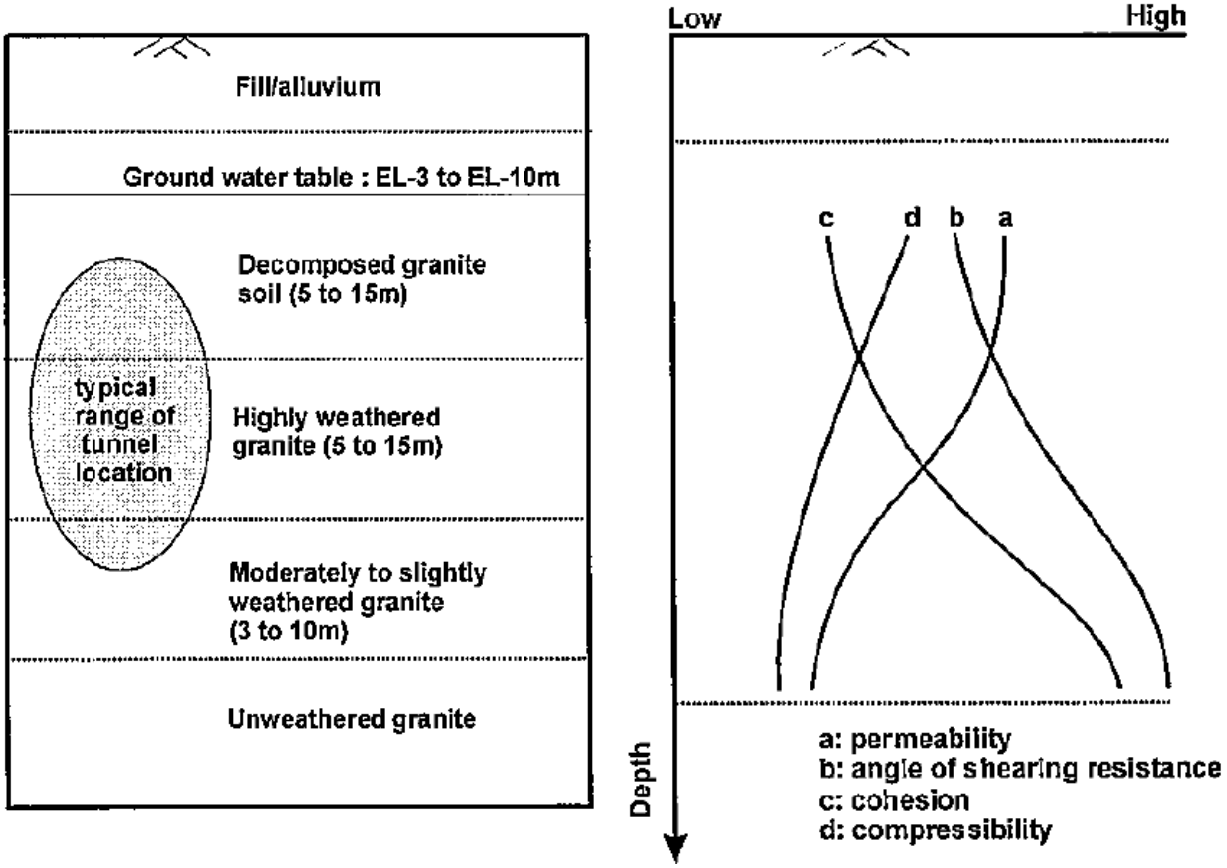
Fig.1 Field measurements of pore-water pressure on a tunnel in silty sand (modified from Inokuma and Ishihara 1995).

1.2 Ground profile

Fig. 2a shows a typical geological profile in the Seoul area, with a subway alignment from 15 to 30 m below the ground surface, therefore engaging different levels of granite weathering at the tunnel face. The weathering reduces with depth, without the development of core stones and the weathering profile is shown in Fig. 2b. The decomposed granite is formed from the in-situ decomposition of the parent rock and has the characteristics of soil. The weathered rock beneath it has the components of residual soils and partly weathered or fresh rock. The engineering properties of in-situ materials vary continuously, as depicted schematically in Fig. 2c.



(a) Soil profile and tunnel alignement



(b) Typical thicknesses of weathering profile, (c) Typical variation of soil properties

Fig. 2 Typical geological profile and tunnel location in the Seoul Subway construction.

2 Numerical model

2.1 Modelling of NATM construction

The key elements involved in the construction of the Seoul Subway are: tunnelling below the groundwater table; mixed-face ground conditions; a noncircular tunnel cross section; tunnels with drainage systems; and tunnels with both a primary and a secondary lining. Numerical modelling of this type of tunnel requires consideration of several geotechnical aspects such as three-dimensional behaviour at the tunnel heading and coupled behaviour between the soil and the groundwater.

The geological profile adopted in the numerical model is shown in Fig. 3. The NATM, using sprayed concrete lining (SCL) or shotcrete, was the main tunnelling method, due its flexibility to accommodate different tunnel shapes in mixed-face ground conditions. A circular and, a more typical, horseshoe shaped tunnel openings in Seoul Subway are investigated through the analyses presented in this paper.

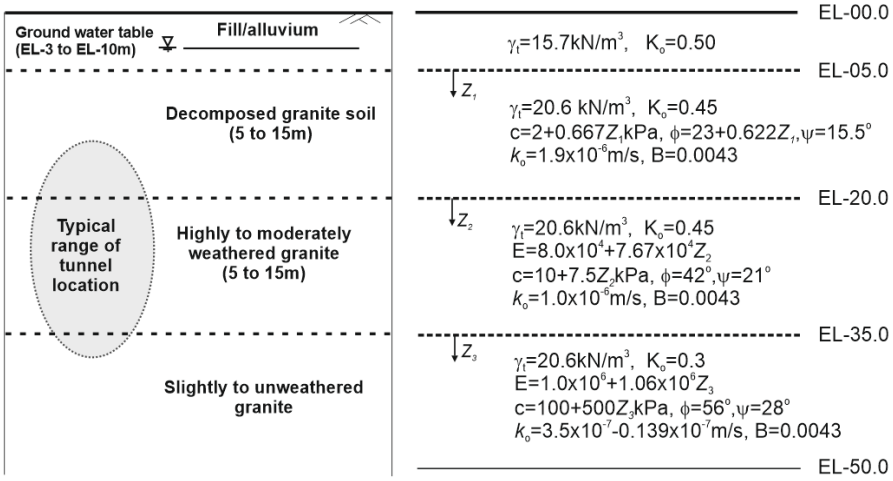


Fig. 3 Ground profile and material properties. γ_t – saturated bulk unit weight; c – cohesion; ϕ – angle of shearing resistance; ψ – angle of dilation.

A large part of the Seoul Subway incorporates design concept of primary and secondary lining. The primary lining includes not only shotcrete but also a wire mesh and steel support and is considered as the primary support system that resists and redistributes external loads. Secondary lining is constructed much later, hence its load-bearing capacity is considered negligible.

The typical excavation advance rate of the tunnel heading during Seoul Subway construction was approximately 2 m/day. Considering the 3D effects of real tunnel construction and that the time-related response of decomposed granite is reasonably fast (a few months) due to its higher permeability, as summarised in Fig. 3 (1.0E-6 to 1E-7 m/s), the implication is that the effect of ground water movement occurs concurrently with tunnel excavation. Based on Shin and Potts (2002), who developed a procedure for 2D modelling of the actual 3D tunnelling process, the 2D hydro-mechanically coupled analyses in the current study adopted the excavation time $T = 15$ days as equivalent of a 2.0 m/day tunnel advance rate. This results into the time for lining installation in the analysis of $t^* = 0.459T$.

Excavation in the analyses is simulated by removing the finite elements representing the soil within the tunnel. The software evaluates the stresses that these elements apply to thetunnel excavation boundary, converts them to equivalent nodal forces, and then applies these in the reverse direction over several increments (i.e., time steps) of the analysis, together with the actual removal of these elements from the mesh (see Potts and Zdravkovic 1999).

2.2 Modelling of lining permeability and drainage system

While it is a common assumption that most tunnels act as drains at some point in time (Ward and Pender 1981), the mechanics of water flow through a concrete lining is a complex phenomenon. Such a flow, strictly, involves seepage, diffusion and sorption. In this paper the main concern is seepage, hence only this aspect is considered. The flow around a tunnel depends on its lining permeability and any drainage system that defines the hydraulic boundary conditions. The approach for realistic modelling of flow through lining developed in this paper, combines beam elements with appropriate

structural stiffness to represent the structural primary lining, and thin solid elements around the lining that have pore pressure degree of freedom and are therefore permeable. The detail of this discretisation in a finite element (FE) mesh is shown in Fig. 4. The permeability of these elements at the start of analysis is equal to the permeability of the surrounding soil. After tunnel excavation and installation of the beam-element lining, this single layer of solid elements is assigned the permeability of the lining. The secondary lining is not considered in the analyses reported here, as its structural capacity is neglected.

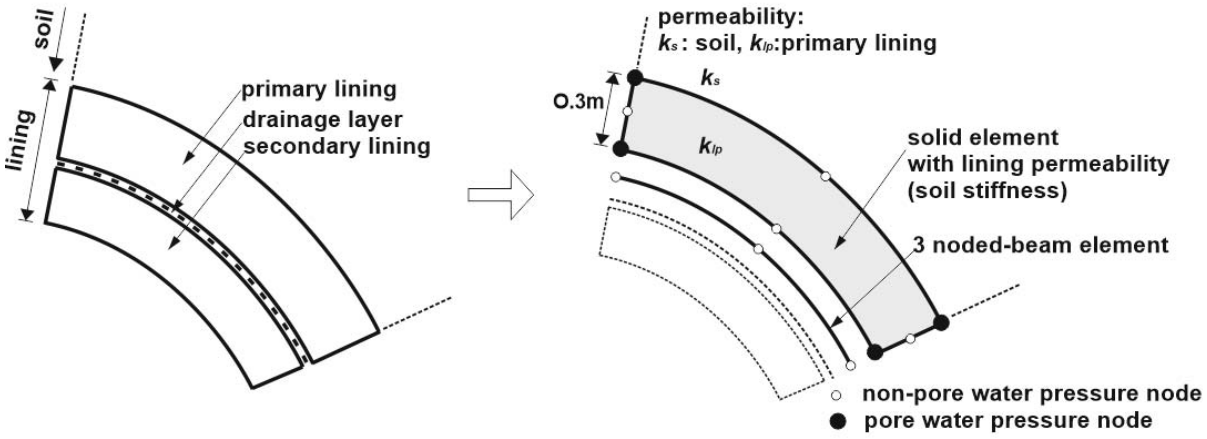


Fig. 4 Modelling of the NATM lining with a drainage system.

3 Finite element analysis

Hydro-mechanically coupled 2D finite elements analyses in the paper were performed with the Imperial College Finite Element Program (ICFEP, Potts and Zdravkovic 1999, 2001), adopting a modified Newton-Raphson scheme with an error-controlled sub-stepping stress-point algorithm as a nonlinear solver.

3.1 Ground profile and constitutive modelling

Fig. 5 shows close up details of FE meshes around analysed tunnel geometries. The soil domain was discretised with 8-noded isoparametric solid continuum elements and the tunnel lining with 3-noded beam elements, as discussed earlier. A 4m diameter circular tunnel represents a typical analysis to be compared against the same tunnel geometry in different ground conditions. The 8.2 m horse-shoe shaped tunnel is typical in Seoul Subway, while the equivalent 9.2m diameter circular tunnel is analysed for comparison of the two geometries.

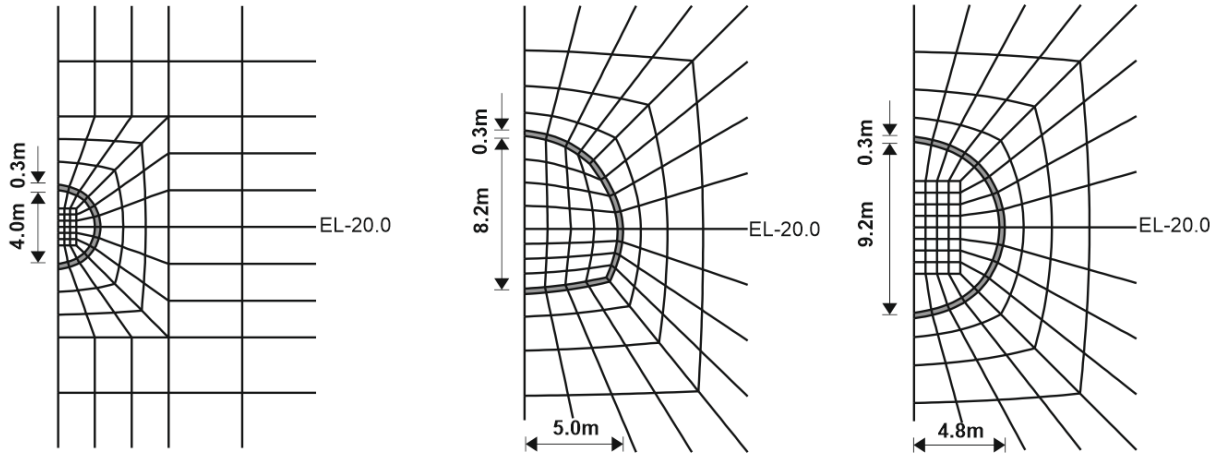


Fig. 5 Finite element models and dimension of analysed tunnels.

The spring-line elevation of all tunnel geometries is at 20.0 m depth. The soil layer above spring-line to the ground surface is the decomposed granite, while the layer below, to the bottom of the mesh, represents the moderately weathered granite. The ground water level was 2.5 m below the ground surface, as depicted in Fig. 3. The soil mechanical behaviour was simulated with a nonlinear Mohr-

Coulomb model, comprising the Mohr-Coulomb yield surface and a nonlinear small strain overlay model. The adopted soil properties from site investigation are summarised in Fig. 3. The NATM sprayed concrete lining was modelled as linear elastic.

3.2 Modelling of permeability

The permeability of the ground was modelled with the nonlinear permeability model proposed by Vaughan (1989), where permeability, k, varies with mean effective stress, $k = k_0 \exp(b \cdot p')$, $k_0$being the permeability at zero mean effective stress and b is a fitting parameter. The permeability model parameters are also summarised in Fig. 3. The permeability of sprayed concrete depends on the water-cement ratio (Neville 1995) and for the usual 0.3-0.55 range the permeability typically varies from 1.0×10^{-10} to 1.0×10^{-12} m/s. Similar to soils, this intact permeability is not usually relevant, as the bulk permeability is influenced by cracks and construction gaps, as more readily available paths for water ingress. Consequently, the evaluation of lining permeability is challenging. In practice, the rate of flow into a tunnel and pore-water pressure acting on the lining will be dependent on the relative permeability of the lining to the adjacent soil. Therefore, the relative permeability of the lining to the soil, k_l/k_s, where k_l is the coefficient of permeability of the lining and k_s is the coefficient of permeability of the soil at the level of the tunnel spring line (based on the initial mean effective stress p' before tunnel construction), could be more important than the absolute value of permeability itself.

3.3 Initial and boundary conditions

In terms of initial stresses, the pore water pressure was assumed hydrostatic with depth from the phreatic surface at 2.5 m below ground level, and zero above the phreatic surface. The initial vertical and horizontal effective stresses were determined from this pore pressure profile and the bulk unit weight and K_0 values given for each layer in Fig. 3.

The mechanical boundary conditions prescribed zero horizontal displacements on the vertical axis of symmetry and on the right hand side vertical boundary of the finite element mesh, while both the vertical and horizontal displacements were set to zero on the bottom boundary of the mesh. The appropriate hydraulic boundary conditions at the tunnel boundary were selected to reflect the desired flow conditions. A fully permeable boundary was modelled by prescribing the pore-water pressure on the excavation boundary as zero, while an impermeable boundary was modelled by prescribing the flow rate as zero. A partially permeable lining was represented by prescribing an appropriate lining permeability and the pore-water pressure on the excavation boundary as zero. The vertical axis of symmetry and the bottom boundary of the mesh were prescribed as no flow boundaries (impermeable), while on the right hand side vertical boundary the pore pressures were assumed not to change from their initial values.

3.4 Analysed cases

A 4m diameter tunnel (Fig. 5) was analysed with the objective of quantifying the pore water pressure contribution to ground loading against typical tunnel construction in London Clay, as a much less permeable soil. A horseshoe shaped tunnel of 8.2 m height and 10.6 m width was analysed as a typical shape on the Seoul Subway. To investigate the effect of tunnel shape, an equivalent 9.2 m diameter circular tunnel was also analysed, having the same cross-sectional area of 66.5 m^2.

4 Results and discussion

Results from the analyses are presented in terms of long-termpore-water pressures (i.e. after full equalisation). These are considered at the outer boundary of the tunnel lining, 0.3 m away from the excavated surface of the tunnel. The potential effects are considered in terms of ground loading and lining performance (i.e. hoop thrust and bending moment). Ground loadings are total normal stresses acting on the lining and consist of effective stress and pore water pressure components. Therefore, the relative contribution of pore water pressure to the ground loading is also considered. Figure 6 defines the ground loading and the pore water pressure and also defines the latter as percentages of the ground loading and of the overburden stress at tunnel axis level.

4.1 Typical analysis

Fig. 7 shows the development of pore water pressure on a tunnel lining in decomposed granite soil, for the 4 m diameter tunnel. Two extreme cases for the hydraulic boundary condition at the tunnel excavation boundary were considered: fully permeable and impermeable. Decomposed granite soil is

sufficiently permeable to give negligible unbalanced (or excess) pore-water pressure at the end of tunnel excavation. The long-term condition is reached reasonably fast. Fig.7 presents the long-term pore-water pressure distribution along a vertical line above the tunnel crown and along a horizontal line at the level of the tunnel spring line. As expected for the fully permeable lining, pore water pressure on the lining is zero, while for the impermeable lining the initial hydrostatic pore water pressure is maintained.

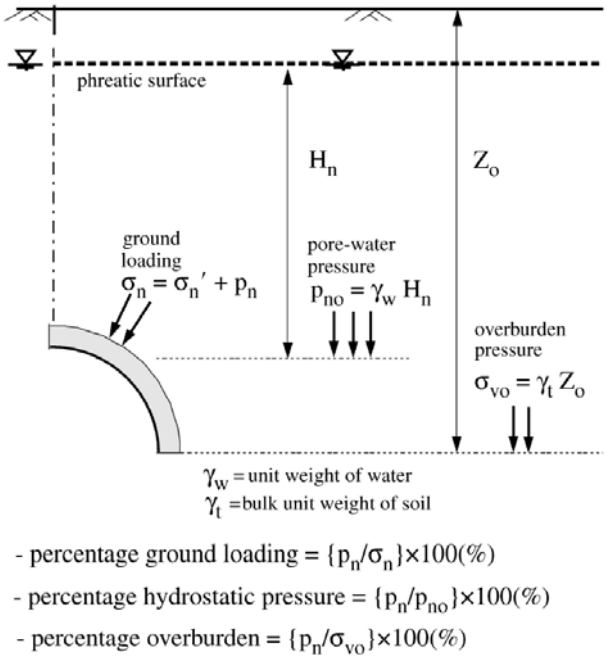


Fig. 6 Quantities used to define pressures on tunnel lining.

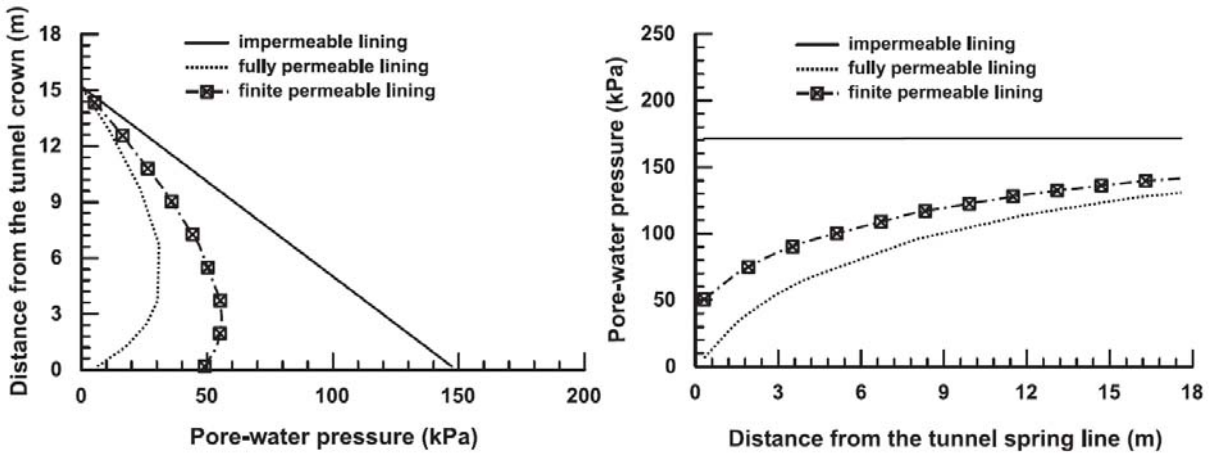


Fig. 7 Long-term pore water pressure: left – above the tunnel crow; right – horizontally along the spring line.

The above results are interpreted in terms of pressures acting on the tunnel lining and are depicted in polar diagrams in Fig. 8. The distribution of the pore water pressure (left) on a fully permeable lining shows zero lining load, while that on an impermeable lining is close to the ground load (as evaluated according to Fig. 6). Calculated as a percentage of the ground loading (Fig. 8 right), the pore pressure on an impermeable lining contributes at 90%.

The effect of finite lining permeability in this analysis is examined with a magnitude of lining permeability $k_l = 1.0 \times 10^{-7}$ m/s, assuming that it is 10 times lower than the permeability of the soil, i.e $k_l/k_s = 0.1$. The results in Fig. 7 and Fig. 8 plot in between the two extreme cases of lining permeability. A pore water pressure of approximately 50 kPa has developed on the lining around the tunnel, comprising around 30% of ground loading. Clearly, this distribution is dependent on the magnitude of the actual lining permeability, k_l.

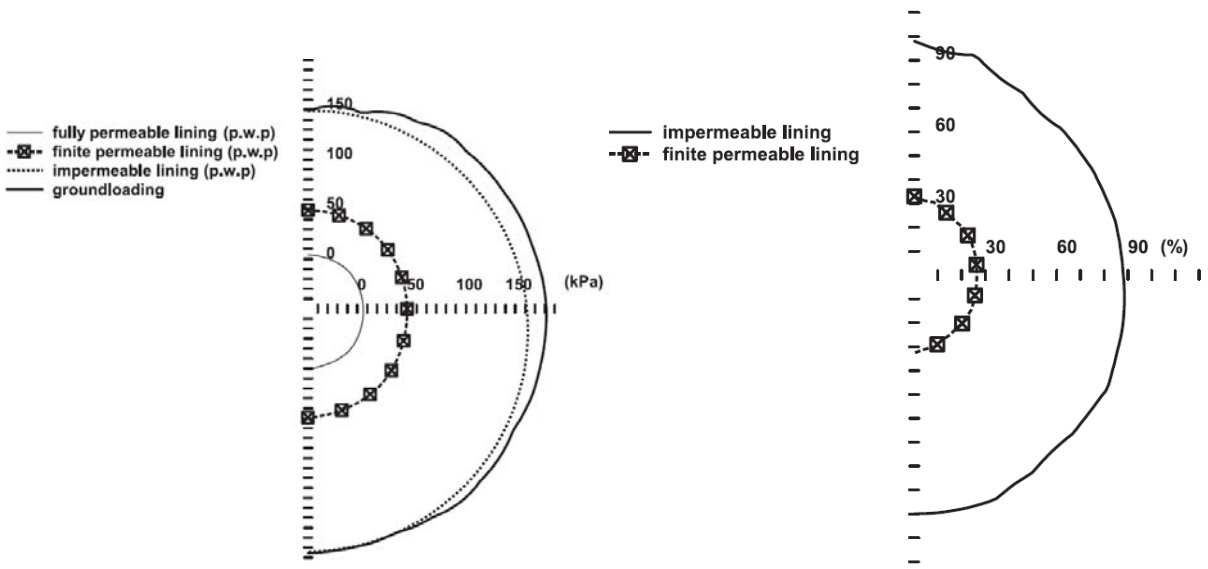


Fig. 8 Long-term loads on lining: left – pore water pressure; right – pore water pressure as percentage of ground loading.

4.2 Comparison with a low permeability soil

In this section, the above results obtained for permeable decomposed granite ground conditions are compared against those obtained from the analysis adopting London Clay ground conditions. This clay has a much lower permeability but higher stiffness due to its overconsolidated state. The analysis of Shin et al. (2002) adopted the same 4.0 m diameter and 20 m spring line depth tunnel geometry.

Only the case of a tunnel with an impermeable lining is considered here. Contrary to decomposed granite, significant pore pressure changes in London clay continue to occur in the long-term after tunnel construction, as depicted in Fig. 9. The long-term distribution of pore water pressures around the tunnel for both soils is the same (Fig. 10 left), however, the ground loading for London clay is larger. The reason for this is that under impermeable lining conditions, swelling takes place in the long term and increases the total stress acting on the lining. Fig.10-right presents the distribution of pore-water pressure as a percentage of ground loading, showing that in London clay, the proportion of pore-water pressure is about 70% of the ground loading at the tunnel spring line, whereas in the decomposed granite soil it is about 90% (similar to the field data shown in Fig. 1). Consequently, the percentage contribution of pore-water pressure to ground loading is dependent on soil type and increases with an increase in soil stiffness.

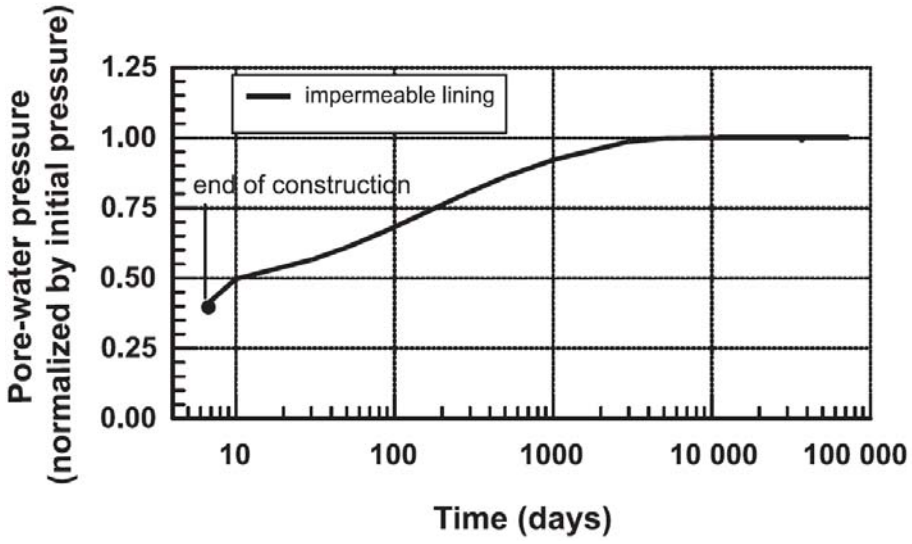


Fig. 9 Long-term evolution of pore water pressure in London clay at the tunnel crown.

4.3 Design considerations for a secondary lining

The implications of the drainage system operation in the primary lining have consequences on the pressures acting on the secondary lining. If blockage of seepage routes in the primary lining happens

in the long term, it has the effect of reducing the permeability of the lining, therefore pore water pressures will develop and act on the lining. In addition, clogging of the drainage filter system would result in the development of water pressures also acting on the secondary lining (Poscher and John 1993).

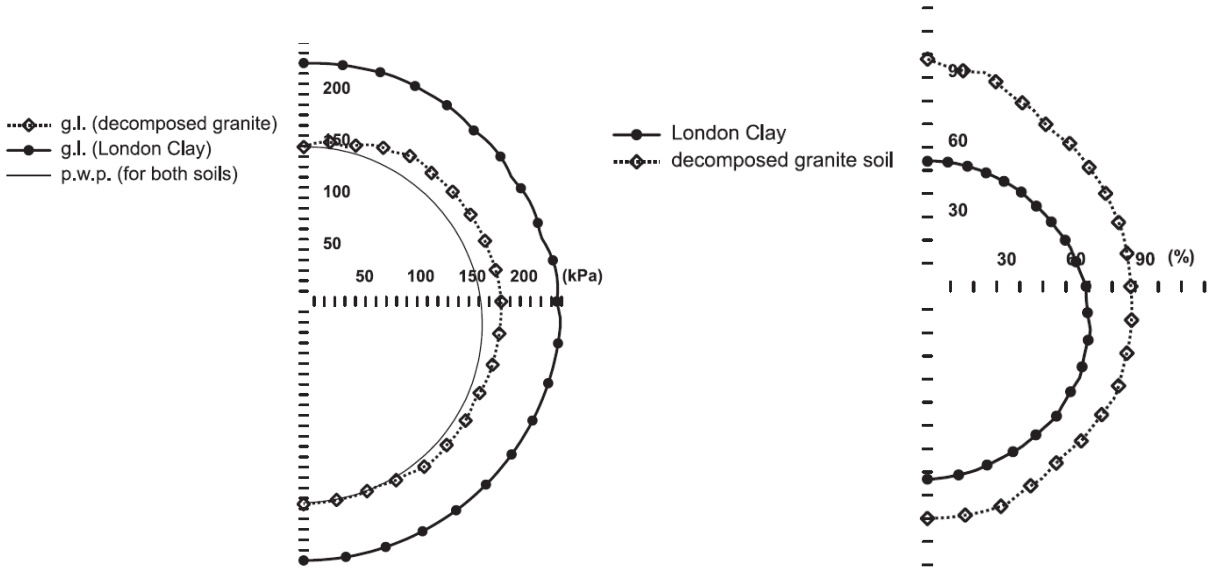


Fig. 10 Comparison of different soil types: left – pore water pressure; right – ground loading.

Not many references in the literature are concerned with loadings on secondary linings. However, as reported insome failure cases (Ferreira 1995; Lee et al. 1996), the most obvious source of loads on the secondary lining would bethe build-up of pore water pressures. In the continuation of this numerical study, the deterioration of the drainage system is achieved by reducing the lining permeability, with assumptions depicted in Fig. 11. The relative permeability between the soil and the drainage system (filter) is considered, as pore-water pressure development is influenced by the relative permeability. Analyses were performed for the tunnel in decomposed granite soil with permeability ratios k_f/k_s varying from 1 to 0.001, where k_f is the permeability of the drainage system (filter), and k_s is the permeability of the soil at the level of the tunnel spring line. It is assumed that the permeability of the primary lining is the same as that of the adjacent soil ($k_s = 1.9 \times 10^{-6}$ m/s).

Figure 14*a* presents the resulting pore-water pressure.

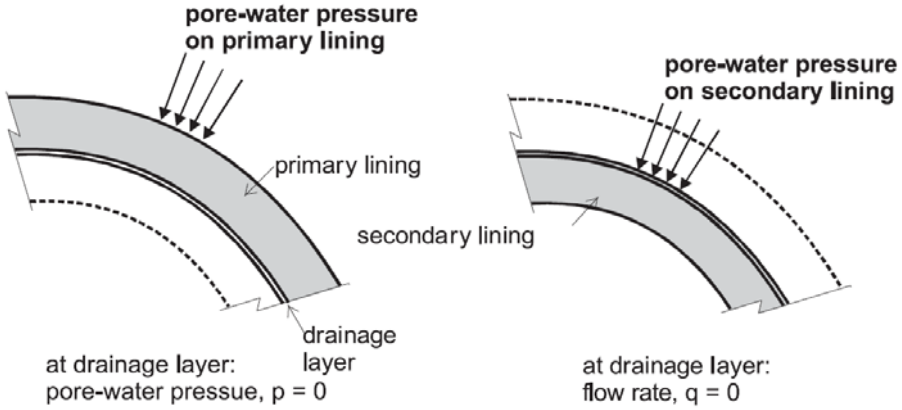


Fig. 11 Potential effect of water pressure: left – drainage system working properly; right – blocking of drainage system.

To quantify the magnitude of pore-water pressure generated due to a decrease in filter permeability, the long-term pore water pressures, p_n, on the lining are normalised by the initial hydrostatic pore-water pressure, p_{no}, (see Fig. 6) and plotted against the permeability ratio k_f/k_s. A single representative curve is obtained from interpretations at several points around the tunnel and is shown in Fig. 12. It is worth noting that the pore pressure increase is significant. Up to 80% of the initial pore water pressure builds up on the secondary lining if filter permeability reduces from $k_f/k_s = 1.0$ to $k_f/k_s = 0.001$. Figure 12 can be used to evaluate the magnitude of pore water pressure evolution on

the secondary lining, if the magnitude of the reduction in filter permeability can be appropriately estimated.

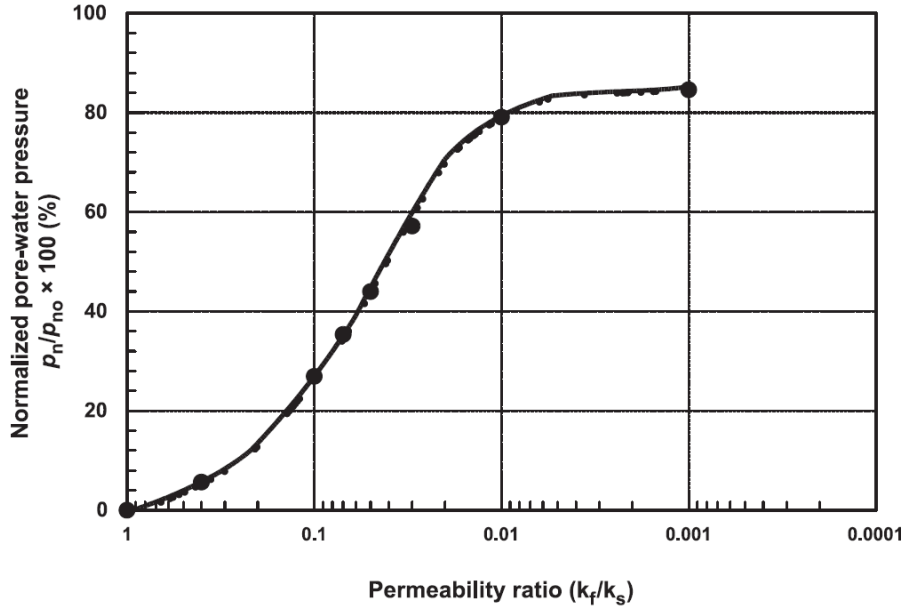


Fig. 12 Variation of pore water pressure loads on secondary lining vs. permeability of the drainage system.

5 Impact on non-circular NATM tunnels

The study on a circular tunnel presented so far indicated that although the magnitude of pore water pressure on tunnel lining can be high, there was little possibility of tensile stresses developing in the lining. However, NATM tunnels in the Seoul Subway are predominantly horseshoe shaped and can therefore be susceptible to high bending moments and associated tensile stresses. The numerical analyses presented in this section are performed on one such cross-section, 8.2 m high and 10.6 m wide, in the same ground conditions as the above analyses of a circular tunnel.

Four scenarios were considered for the hydraulic boundary condition at the tunnel: fully permeable, finite permeability ($k_l/k_s = 0.1$ and 0.01); and impermeable lining. Fig. 13 shows distributions of ground loading and pore pressure on the lining. The peak value of ground loading occurs at the location of the corner of the horseshoe cross-section, where $\theta = -30^o$, and it increases from 400 kPa for a fully permeable lining to 440 kPa for an impermeable lining. The location of the peak value moves upward with the decrease in lining permeability. The contribution of the pore water pressure to the ground loading varies significantly with location around the lining and increases with the decrease in lining permeability, as shown in Fig. 14.

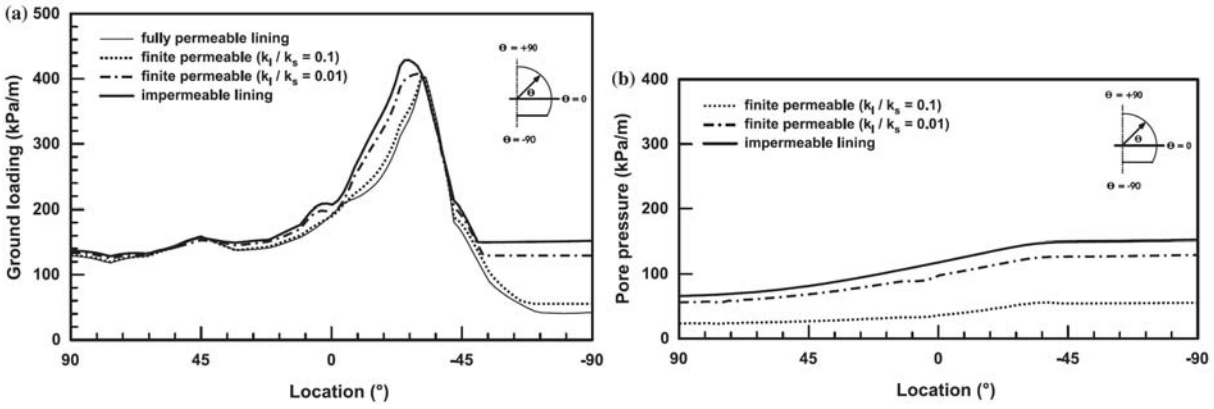


Fig. 13 Pressures on primary horseshoe shape lining: left – ground loading; right – pore pressure.

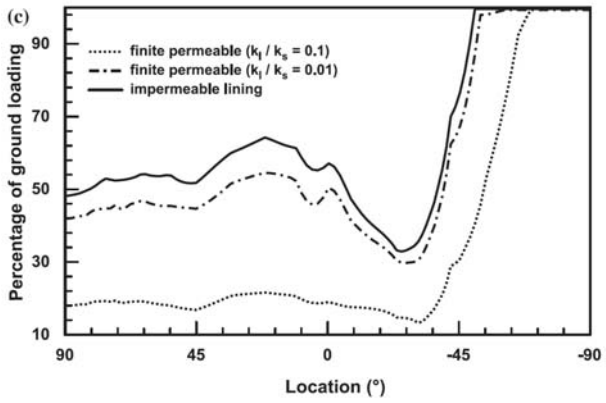


Fig. 14 Pore pressure as percentage of ground loading on a primary horseshoe shaped lining.

The effect of pore-water pressure on lining performance was also investigated. Although the differences in ground loadings, as indicated in Fig. 13, do not appear to be large, significant changes in hoop thrust and bending moment were induced in the tunnel wall and invert, as shown in Fig. 15. A decrease in lining permeability results in a significant increase in the hoop thrust and in the bending moment below the tunnel spring line. The maximum hoop thrust and bending moment occurred in the impermeable lining. A thrust of 900 kN/m occurred at around the spring line, and abending moment of 300 kN·m/m occurred at the corner ofthe lining, at $\theta = -30^{o}$. This maximum bending moment is approximately 100% larger than that obtained for the permeable lining.

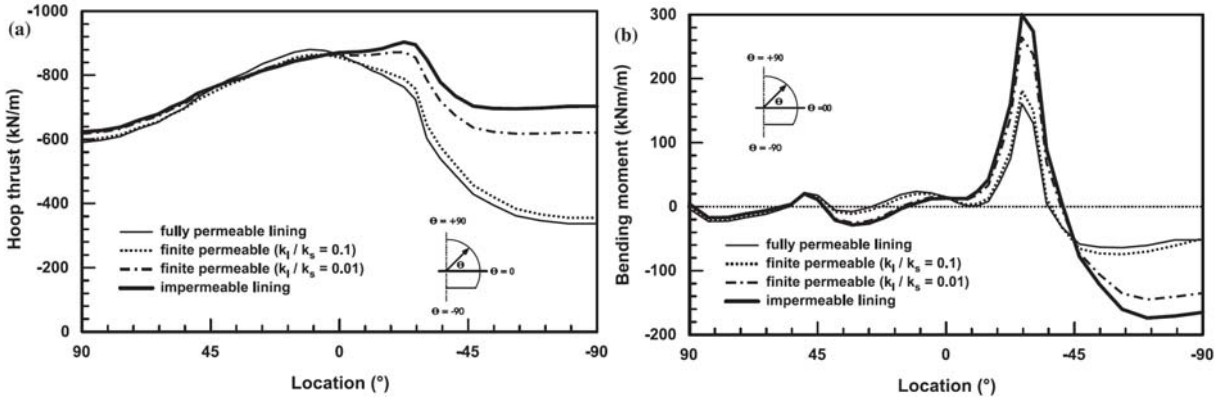


Fig. 15 Response of a primary horseshoe shaped lining: left – hoop thrust; right – bending moment.

If clogging occurs in the drainage layer between the primary and the secondary lining, the pore pressures shown in Fig. 13 would act on the secondary lining. The performance of the secondary lining due to such pore-water pressures is presented in Fig. 16, which shows the distribution of maximum principal stress (tension positive), predicted to occur between the tunnel spring line and the corner. As expected, the magnitude of tensile stress increases as the permeability of the drainage layer reduces and demonstrates that excessive bending distortion, as a direct result of degradation of the drainage layer, in a horseshoe-shaped tunnel could lead to unacceptable tensile stresses in the secondary lining.

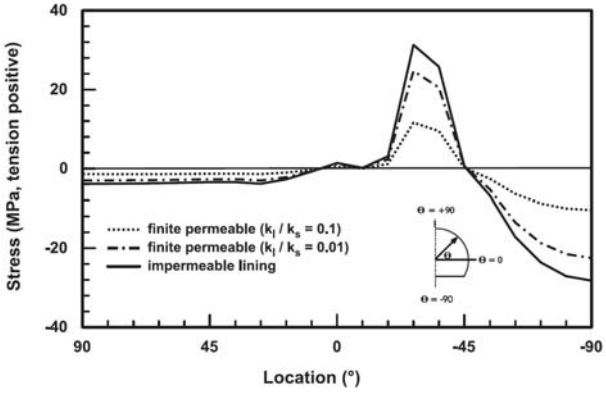


Fig. 16 Maximum principal stress in a secondary lining due to pore water pressure (tension +ve).

Shin et al. (2005) examined these predictions against some known failure cases, notably the failure of the secondary lining on the Seoul Subway (Lee et al. 1996) and a similar failure in the Carvalho Pinto Road tunnel in Brazil (HSE 1996). In both cases only the secondary lining was affected, developing long cracks parallel to the tunnel axis between the spring line and the corner (θ from 0^o to -30^o), due to the pore pressure loading. Those observations were in the location of the tensile stress predicted in Fig. 16.

In the construction of the Seoul Subway, the majority of the ground conditions warranted the use of a horseshoe shaped tunnel. Shin and Potts (2002) highlighted that in decomposed granite, due to its significant increase of stiffness with depth, a horseshoe-shaped tunnel was structurally more beneficial than a circular tunnel. However, this benefit would reduce if the lining loads from pore-water pressure were considerable, particularly for the secondary lining. To quantify the effect of tunnel shape, an analysis was performed of a circular tunnel with a secondary lining and with the same cross-section area of the horseshoe shape tunnel, and the results compared. Geological conditions, tunnel depth and modelling details were the same for the two tunnels. Fig. 17 compares the distribution of ground loading and pore pressure for the case of $k_l/k_s = 0.1$. Although the predicted pore pressures on a circular lining are higher than on the horseshoe shaped lining in the upper part of the tunnel, the pore pressure contribution to ground loading varies between 30 and 40% for the former lining and between 15 and 100% for the latter. Regarding the behaviour of the secondary lining due to pore water pressure loading on the circular tunnel, the effect is negligible as the maximum principal stress is everywhere compressive. The lower part of the horseshoe shaped tunnel, however, develops tensile stress. This indicates that the time dependency of the permeability due to degradation of the drainage system should be considered when designing non-circular tunnels.

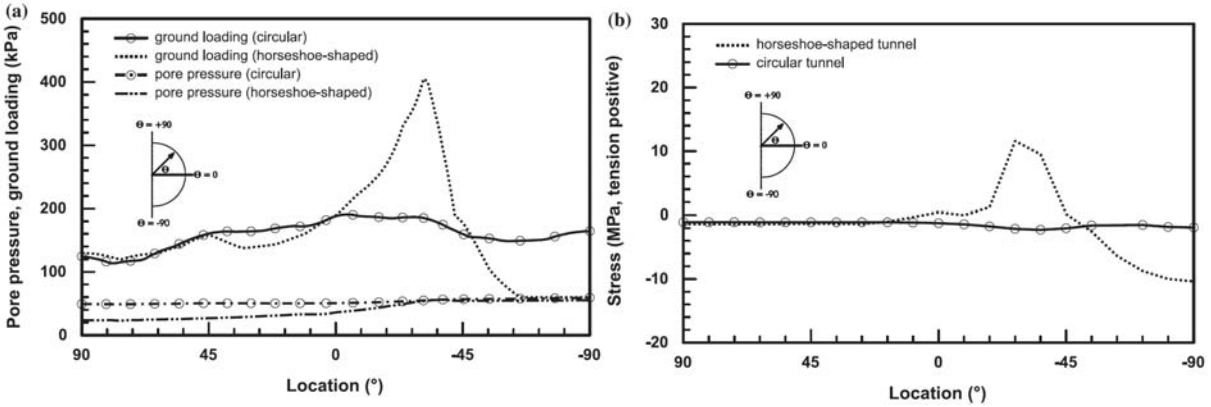


Fig. 17 The effect of tunnel shape: left-pore pressure and ground loading; right-secondary lining performance.

6 Conclusions

The study presented in this paper reveals the complexity of NATM tunnelling below the ground water level, in mixed ground conditions of a weathering rock. Through the robust numerical model, which was shown to predict reliably the field observations, the following are identified as key outputs:

- The majority of the ground loading on a tunnel in a weathered rock arises from pore water pressure, if the lining is impermeable;
- Changes in lining permeability change the contribution of the pore water pressure to ground loading, without changing the magnitude of ground loading;
- The magnitude of the pore water pressure on the lining is dependent on the relative permeability of soil to lining, k_l/k_s; as this ratio decreases, the pore pressure increases.

It was also highlighted that tunnel shape has a strong impact on the lining stresses resulting from external water pressure. Numerical analysis of a non-circular NATM tunnel revealed that the development of residual pore-water pressures could cause significant detrimental effects on a secondary lining in the long term. Excessive bending distortion in a noncircular tunnel could lead to unacceptable cracking in the lining and ultimate lining failure.

It is recommended that the time dependency of lining permeability due to the deterioration of the drainage system should be considered as a critical factor in lining design, particularly for a secondary

lining, which is usually not designed to cope with pore-water pressure loading. By performing a parametric study for a tunnel with different lining permeabilities, a design curve is proposed to help evaluate the likely pore-water pressure loads on a secondary lining in decomposed granite ground conditions.

References

Ferreira AA (1995) Cracks and repairing of the Carvalho PintoRoad Tunnel (Brazil). Exchange of correspondence with Healthand Safety Executive, UK (in 1996).

Hajra MG, Reddi LN, Glasgow LA, Xiao M, Lee IM(2002) Effects of ionic strength on fine particle clogging of soilfilters. Journal of Geotechnical and Geoenvironmental Engineering,**128**(8): 631–639.

HSE (1996) Safety of new Austrian tunnelling method (NATM)tunnels, a review of sprayed concrete lined tunnels with particularreference to London Clay. Health and Safety Executive(HSE) UK.

Inokuma A, Ishimura T(1995) Earth pressure acting on shield driven tunnels in soft ground. *In p*roceedings of the InternationalConference on Underground Construction in SoftGround, New Delhi, India, A.A. Balkema, Rotterdam, TheNetherlands, pp. 221–224.

Lee YN, Byun HK, Shin OJ (1996) Cracking of subwaytunnel concrete lining and its repair. *In* Proceedings of the NorthAmerican Conference Nat '96 and 22nd General Assembly InternationalTunnelling Association, Washington, D.C., 21–24A.A. Balkema, Rotterdam, The Netherlands,pp. 325–329.

Neville AM (1995) Properties of concrete, 4th ed., LongmanGroup Limited, Malaysia.

O'Rourke TD (1984). Guidelines for tunnel lining design. AmericanSociety of Civil Engineers, Reston, Va.

Parks P, Francis J, Gorlov A, Gorlova E, Guertin JD (1986) Water intrusion problems in transit tunnels. Final Report (UMTA-MA-06-0156-86-1) to US Department of Transportation,UMTA Technical Assistance Program

Peck RB (1969) Deep excavations and tunnelling in soft ground –state of the art. *In* Proceedings of the 7th International Conferenceon Soil Mechanics and Foundation Engineering, State ofthe Art Volume, pp. 225–290.

Poscher G, John M (1993) Experiences gained with measuresdesigned to reduce shotcrete eluations in the tunnels of theVerbingsdungskurveNantenbach. *In* Proceedings of the International Symposiumon Sprayed Concrete, Oslo, pp. 401–415.

Potts DM, Zdravkovic L 2(1999)Finite element analysis in geotechnical engineering: theory; Thomas Telford Publishing, London, UK.

Shin JH, Potts DM (2002) Time-based two dimensionalmodelling of NATM tunnelling. Canadian Geotechnical Journal,**39**: 710–724.

Shin JH, Addenbrooke TI, Potts DM (2002) A numericalstudy of the effect of groundwater movement on long-term tunnelbehaviour. Géotechnique, **52**(6): 391–403.

Shin JH, Potts DM, Zdravkovic L (2005) The effect of pore-water pressure on NATM tunnel linings in decomposed granite soil. Canadian Geotechnical Journal 42, pp 1585-1599,

Vaughan PR (1989)Non-linearity in seepage problems — theoryand field observation. De Mello Volume, Edgard Blucher Ltd.,Sao Paulo, Brazil. pp. 501–516.

Ward WH, Pender MJ (1981) Tunnelling in soft ground–general report. *In* Proceedings of the 10th International Conferenceof Soil Mechanics and Foundation Engineering, Stockholm,Sweden, A.A. Balkema, Rotterdam,The Netherlands. Vol. 4, pp 261–275.